Plane-Geometry Approximation of Image
Fields and Betatron Frequencies for a
Ring Beam with Coaxial Conducting Boundaries

M. Reiser†

IPP

MAX-PLANCK-INSTITUT FÜR PLASMAPHYSIK

8046 GARCHING BEI MÜNCHEN

MAX-PLANCK-INSTITUT FÜR PLASMAPHYSIK

GARCHING BEI MÜNCHEN

Plane-Geometry Approximation of Image
Fields and Betatron Frequencies for a
Ring Beam with Coaxial Conducting Boundaries

M. Reiser†

IPP 0/28   Dec.1975

†University of Maryland, Department of
Physics and Astronomy

IPP 0/28   M. Reiser   Plane-Geometry Approximation of
Image Fields and Betatron Fre-
quencies for a Ring Beam with
Coaxial Conducting Boundaries

Abstract

The fields and gradients due to image charges and image currents
in coaxial conductors inside and outside of a relativistic elec-
tron ring are calculated using a plane-geometry approximation.
In the cases considered one of the conducting boundaries is of
a squirrel-cage type which prevents azimuthal current flow and
thus suppresses the magnetic image fields associated with such
currents. Various combinations (squirrel-cage inside/conductor
outside or vice versa, one conductor only or one squirrel-cage
only either inside or outside of the ring) were studied and the
effects of the image forces on incoherent betatron frequencies
were calculated. Results are compared with exact numerical cal-
culations (involving Bessel functions) by Laslett, Hofmann and
Greenwald.

1. Introduction

The radial and axial betatron frequencies in an electron ring accelerator (ERA) are strongly affected by image forces due to surrounding walls. Without such boundaries, if the electron ring is located in a uniform external magnetic field, no focusing exists in the axial direction. This is still true when coaxial conducting cylinders are present, since the focusing forces are concerned, but to have no effect on the magnetic field due to electrostatic images are essentially cancelled by the defocusing effects of the magnetic image fields. However, if the magnetic images are suppressed, a net focusing effect may exist. This is achieved with the use of a "squirrel-cage" cylinder in which no azimuthal image currents can flow, while electro-static images are practically unaffected.[1]

The use of such a "squirrel cage" to obtain axial focusing is in conflict with the need for a coaxial wall with good azimuthal conductivity to suppress the negative mass instability.[2] In an attempt to cure both problems, one can use a combination of squirrel cage and conducting cylinder, with the squirrel cage inside and the conductor outside or vice versa. The influence on axial focusing and negative mass instability then depends strongly on the relative spacing between the electron ring and the two coaxial boundaries.

Theoretically, the calculation of electric and magnetic fields and gradients in such a geometry is a somewhat tedious problem. Hofmann[3] solved it for the case where the squirrel cage is outside and the conductor inside, and he tabulated the fields and gradients for a number of parameter values. A similar study was done by Greenwald[4] for the case where both inner and outer cylinders are good conductors.

Such exact mathematical solutions with the use of Bessel functions have the disadvantage that one has to resort to lengthy computer calculations or tabulated results. From a practical point of view, however, a simple analytical approximation is often sufficient and more useful to make quick survey-type

calculations in connection with design studies or experiments. This motivated

the analysis presented in this report.

In the model used here, the coaxial cylinders are approximated by coplanar

boundaries and the electron ring by a line charge. This implies that the

separation of the conductors is small compared to the diameter of the electron

ring. The squirrel cage is assumed to be an ideal conductor as far as electric

images are concerned, but to have no effect on the magnetic field. Section 2

treats the electrostatic problem, Section 3 the magnetostatic problem, and

in Section 4 the results are applied to obtain analytical expressions for the

image effects on the betatron frequencies. Complete expressions for the

frequencies are presented in Section 5.

2. Electrostatic Image Fields and Gradients

Consider a line charge of density λ [C/m] situated between two co-planar

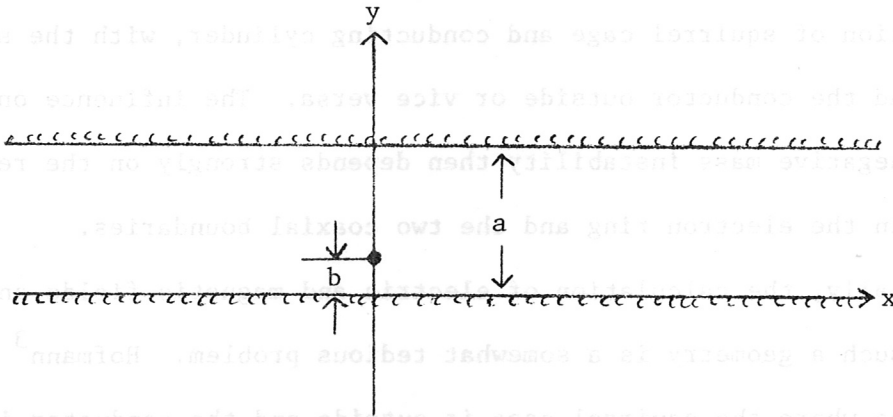conductors as shown in Fig. 1 below.

Fig. 1 Geometry of line charge between conducting
planes.

According to Smythe[5], this problem can be treated by conformal mapping, and

one obtains for the potential function U in the x = 0 plane the following

result (in MKS units):

$$(1) \qquad \tanh \frac{2\pi\varepsilon_o U}{\lambda} = \frac{\sin \frac{\pi b}{a} \sin \frac{\pi y}{a}}{1 - \cos \frac{\pi b}{a} \cos \frac{\pi y}{a}} = X$$

or

$$(2) \qquad U = \frac{\lambda}{2\pi\varepsilon_o} \tanh^{-1} X$$

For the electric field strength in the $x = 0$ plane follows from (2):

$$E_y = -\frac{\partial U}{\partial y} = -\frac{\lambda}{2\pi\varepsilon_o} \frac{1}{1 - X^2} \frac{\partial X}{\partial y},$$

or

$$(3) \qquad E_y = -\frac{\lambda}{2\pi\varepsilon_o} \frac{\pi}{a} \frac{\sin \frac{\pi b}{a}}{\cos \frac{\pi y}{a} - \cos \frac{\pi b}{a}}$$

To obtain the contribution of the image charges to the electric field along the $x = 0$ plane, we subtract from (3) the field due to a free line charge, i.e.,

$$(4) \qquad E_y^i = -\frac{\lambda}{2\pi\varepsilon_o} \left[\frac{\pi}{a} \frac{\sin \frac{\pi b}{a}}{\cos \frac{\pi y}{a} - \cos \frac{\pi b}{a}} + \frac{1}{y - b} \right]$$

By expanding the denominator to fourth order and differentiation, one obtains for the image field, the first and second derivative at $y = b$ the results:

$$(5) \qquad E_y^i \Big/_{y=b} = E^i = -\frac{\lambda}{4\varepsilon_o a} \cot \frac{\pi b}{a}$$

$$(6) \qquad \frac{\partial E^i}{\partial y} = \frac{\lambda}{2\varepsilon_o a} \frac{\pi}{a} \left(\frac{1}{6} + \frac{1}{4} \cot^2 \frac{\pi b}{a} \right)$$

$$(7) \qquad \frac{\partial^2 E^i}{\partial y^2} = -\frac{\lambda}{2\varepsilon_o a} \frac{\pi^2}{a^2} \left[\frac{1}{12} \cot^2 \frac{\pi b}{a} + \frac{1}{4} \cot^3 \frac{\pi b}{a} \right]$$

For completeness, we add the results when only <u>one</u> conductor or a squirrel cage is present.

A. <u>Conductor or squirrel cage inside</u>

$$(8) \qquad E^i = -\frac{\lambda}{4\pi\varepsilon_o b}$$

(9)
$$\frac{\partial E^i}{\partial y} = \frac{\lambda}{8\pi\varepsilon_o b^2}$$

(10)
$$\frac{\partial^2 E^i}{\partial y^2} = -\frac{\lambda}{8\pi\varepsilon_o b^3}$$

B. Conductor or squirrel cage outside

(11)
$$E^i = \frac{\lambda}{4\pi\varepsilon_o b}$$

(12)
$$\frac{\partial E^i}{\partial y} = \frac{\lambda}{8\pi\varepsilon_o b^2}$$

(13)
$$\frac{\partial^2 E^i}{\partial y^2} = \frac{\lambda}{8\pi\varepsilon_o b^3}$$

3. Magnetic Image Fields and Gradients

For the calculation of the magnetic image fields and gradients, we ignore the squirrel cage, i.e., we assume that only one conductor exists, either inside or outside of the electron ring. Let the distance between beam and conductor be b. Furthermore, assume that the magnetic field has not penetrated through the conductor.

A. Conductor inside, squirrel cage outside

In the plane-geometry approximation, the magnetic image field and its first and second derivatives at the position of the beam in the x = 0 plane is given by

$$B_x^i = \frac{\mu_o I}{2\pi(y+b)}$$

or, for y = b,

(14)
$$B^i = \frac{\mu_o I}{4\pi b}$$

(15)
$$\frac{\partial B^i}{\partial y} = -\frac{\mu_o I}{8\pi b^2}$$

(16)
$$\frac{\partial^2 B^i}{\partial y^2} = \frac{\mu_o I}{8\pi b^3}$$

B. Conductor outside, squirrel cage inside

(17)
$$B^i = -\frac{\mu_o I}{4\pi b}$$

(18)
$$\frac{\partial B^i}{\partial y} = -\frac{\mu_o I}{8\pi b^2}$$

(19)
$$\frac{\partial^2 B^i}{\partial y^2} = \frac{\mu_o I}{8\pi b^3}$$

4. Image Contributions to Betatron Frequencies

The radial and axial betatron frequencies are given in terms of the fields and gradients at the equilibrium orbit R as follows:[6]

(20)
$$\nu_r^2 = 1 + \frac{1}{E_r + v_\Theta B_z}\left[E_r + R\frac{\partial E_r}{\partial r} + Rv_\Theta\frac{\partial B_z}{\partial r}\right] + \frac{E_r^2(1-\beta^2)}{(E_r + v_\Theta B_z)^2}$$

(21)
$$\nu_z^2 = \frac{1}{E_r + v_\Theta B_z}\left[R\frac{\partial E_z}{\partial z} - Rv_\Theta\frac{\partial B_r}{\partial z}\right]$$

Here, E_r and B_z are the total electric and magentic fields at the equilibrium orbit R. The last term in (20) is negligibly small in our case and will be ignored subsequently.

For the image contributions, the curl and divergence are zero at $r = R$, i.e.,

(22)
$$\frac{\partial E_z^i}{\partial z} = -\frac{E_r^i}{R} - \frac{\partial E_r^i}{\partial r} \quad \text{and} \quad \frac{\partial B_r^i}{\partial z} = \frac{\partial B_z^i}{\partial r}$$

The E_r term in (20) and (22) is due to the curvature of the beam and boundaries and disappears if one goes to a plane-geometry approximation, as is being done here. We therefore ignore it in the following calculations and write for the changes in ν_r^2 and ν_z^2 due to the image forces:

$$(23) \qquad (\Delta\nu_z^2)_{image} = \frac{1}{E_r + v_\theta B_z} \left[-R \frac{\partial E_r^i}{\partial r} - Rv_\theta \frac{\partial B_z^i}{\partial r} \right] = -(\Delta\nu_r^2)_{image}.$$

Let R_1 be the radius of the inner cylinder, R_2 that of the outer cylinder.

Define the parameters

$$T = \frac{R_1}{R}, \quad S = \frac{R_2}{R}, \quad S - T = \frac{R_2 - R_1}{R} = \frac{a}{R}$$

i.e., $a = R(S - T)$, $b = R(1 - T)$, $\frac{b}{a} = \frac{1 - T}{S - T}$.

Line charge λ and current I for an electron ring with N_e electrons and a fraction $f = N_i/N_e$ of stationary ions are given by

$$(24) \qquad \lambda = -\frac{eN_e(1 - f)}{2\pi R}, \quad I = \frac{eN_e}{2\pi R}\beta c$$

where $\beta c = v_\theta$ is the mean azimuthal velocity of the electrons.

With these parameters and replacing y by r, x by z, one obtains for the image fields and gradients from the plane-geometry approximations the following expressions:

$$(25) \qquad E_r^i = \frac{eN_e(1 - f)}{8\pi^2\epsilon_o R^2} \frac{\pi}{S - T} \cot\pi\frac{1 - T}{S - T}$$

$$(26) \qquad R\frac{\partial E_r^i}{\partial r} = -\frac{eN_e(1 - f)}{8\pi^2\epsilon_o R^2} \frac{\pi^2}{2(S - T)^2}\left[\frac{2}{3} + \cot^2\pi\frac{1 - T}{S - T}\right]$$

$$(27) \qquad R^2\frac{\partial^2 E_r^i}{\partial r^2} = \frac{eN_e(1 - f)}{8\pi^2\epsilon_o R^2} \frac{\pi^3}{2(S - T)^3}\left[\cot^3\pi\frac{1 - T}{S - T} + \frac{1}{3}\cot\pi\frac{1 - T}{S - T}\right]$$

A. Squirrel cage outside, conductor inside

$$(28) \qquad v_\theta B_z^i = -\mu_o\frac{eN_e v_\theta^2}{8\pi^2 R^2(1 - T)} = -\frac{eN_e}{8\pi^2\epsilon_o R^2}\frac{\beta^2}{1 - T}$$

$$(29) \qquad Rv_\theta\frac{\partial B_z^i}{\partial r} = \frac{eN_e}{8\pi^2\epsilon_o R^2}\frac{\beta^2}{2(1 - T)^2}$$

$$(30) \quad R^2 v_\Theta \frac{\partial^2 B_z{}^i}{\partial r^2} = - \frac{eN_e}{8\pi^2 \epsilon_o R^2} \frac{\beta^2}{2(1-T)^3}$$

B. Squirrel cage inside, conductor outside

$$(31) \quad v_\Theta B_z{}^i = \frac{eN_e}{8\pi^2 \epsilon_o R^2} \frac{\beta^2}{S-1}$$

$$(32) \quad R v_\Theta \frac{\partial B_z{}^i}{\partial r} = \frac{eN_e}{8\pi^2 \epsilon_o R^2} \frac{\beta^2}{2(S-1)^2}$$

$$(33) \quad R^2 v_\Theta \frac{\partial^2 B_z{}^i}{\partial r^2} = \frac{eN_e}{8\pi^2 \epsilon_o R^2} \frac{\beta^2}{2(S-1)^3}$$

C. One conductor inside

$$(34) \quad E_r{}^i - v_\Theta B_z{}^i = \frac{eN_e}{8\pi^2 \epsilon_o R^2} \frac{1}{1-T} (1-f-\beta^2)$$

$$(35) \quad R \frac{\partial E_r{}^i}{\partial r} + R v_\Theta \frac{\partial B_z{}^i}{\partial r} = - \frac{eN_e}{8\pi^2 \epsilon_o R^2} \left[\frac{1}{2(1-T)^2} (1-f-\beta^2) \right]$$

$$(36) \quad R^2 \frac{\partial^2 E_r{}^i}{\partial r^2} + R^2 v_\Theta \frac{\partial^2 B_z{}^i}{\partial r^2} = \frac{eN_e}{8\pi^2 \epsilon_o R^2} \frac{1}{2(1-T)^3} (1-f-\beta^2)$$

D. One conductor outside

$$(37) \quad E_r{}^i - v_\Theta B_z{}^i = - \frac{eN_e}{8\pi^2 \epsilon_o R^2} \frac{1}{S-1} (1-f-\beta^2)$$

$$(38) \quad R \frac{\partial E_r{}^i}{\partial r} + R v_\Theta \frac{\partial B_z{}^i}{\partial r} = - \frac{eN_e}{8\pi^2 \epsilon_o R^2} \left[\frac{1}{2(S-1)^2} (1-f-\beta^2) \right]$$

$$(39) \quad R^2 \frac{\partial^2 E_r{}^i}{\partial r^2} + R^2 v_\Theta \frac{\partial^2 B_z{}^i}{\partial r^2} = - \frac{eN_e}{8\pi^2 \epsilon_o R^2} \frac{1}{2(S-1)^3} (1-f-\beta^2)$$

E. Only a squirrel cage is present

In this case, no magnetic image contributions exist and the electric fields and gradients are obtained by setting $\beta^2 = 0$ in Eqs. (34) to (39).

From the force-balance equation, one gets

$$\frac{\gamma m_o v_\theta^2}{R} = e(E_r + v_\theta B_z)$$

or

(40)
$$E_r + v_\theta B_z = \frac{\gamma m_o \beta^2 c^2}{eR}$$

Furthermore, we can write

(41)
$$\frac{eN_e}{8\pi^2 \varepsilon_o R^2} \frac{1}{E_r + v_\theta B_z} = \frac{N_e}{2\pi R} \frac{e^2}{4\pi\varepsilon_o m_o c^2} \frac{1}{\gamma\beta^2} = \frac{\nu}{\gamma\beta^2}$$

Here we introduced the Budker parameter ν which is the product of particle line density $\frac{\lambda}{e} = \frac{N_e}{2\pi R}$ and classical electron radius $r_e = \frac{e^2}{4\pi\varepsilon_o m_o c^2}$. The image contributions to the betatron frequencies are then obtained by substituting the approximate results for the fields and gradients into Eq. (23) using the relation (41). The results may then be written in the following form:

(42)
$$(\Delta\nu_z^2)_{image} = - (\Delta\nu_r^2)_{image} = \frac{\nu}{\gamma} \Delta_i .$$

For the parameter Δ_i, one gets the following expressions.

A. Conductor and squirrel cage

(43)
$$\Delta_i = \frac{\pi^2 (1-f)}{2\beta^2 (S-T)^2} \left(\frac{2}{3} + \cot^2 \pi \frac{1-T}{S-T}\right) - \frac{1}{2(1-S_M)^2}$$

$$\text{where } S_M = \begin{cases} T & \text{when S.C. outside, conductor inside} \\ S & \text{when S.C. inside, conductor outside} \end{cases}$$

B. Squirrel cage only, outside

(44)
$$\Delta_i = \frac{1-f}{2\beta^2 (S-1)^2}$$

C. Squirrel cage only, inside

(45)
$$\Delta_i = \frac{1 - f}{2\beta^2 (1 - T)^2}$$

D. Conductor only, outside

(46)
$$\Delta_i = \frac{1 - f - \beta^2}{2\beta^2 (S - 1)^2}$$

E. Conductor only, inside

(47)
$$\Delta_i = \frac{1 - f - \beta^2}{2\beta^2 (1 - T)^2}$$

To check the accuracy of our analytical approximation, we compare the electric image fields and gradients according to Eqs. (25) and (26) with the exact numerical results obtained by Greenwald[4] for a few values of the parameters S and T. With the definitions

$$E_r^{\ i} = \frac{eN_e}{4\pi\epsilon_o R^2} k_e \ , \qquad R \frac{\partial E_r^{\ i}}{\partial r} = \frac{eN_e}{4\pi\epsilon_i R^2} k_r \ ,$$

we have the approximate expressions from (25) and (26):

$$k_e = \frac{1}{2(S - T)} \cot \pi \frac{1 - T}{S - T} \ , \qquad k_r = - \frac{\pi}{4(S - T)^2} \left(\frac{2}{3} + \cot^2 \pi \frac{1 - T}{S - T} \right) .$$

Table 1

T	S	k_e Eq. (25)	k_e Greenwald	k_r Eq. (26)	k_r Greenwald
0.95	1.05	0	0.61	−52.36	−50.50
	1.10	1.98	2.47	−34.91	−36.17
	1.20	2.75	3.28	−32.18	−34.25
	1.40	3.05	3.57	−31.86	−34.22
0.90	1.10	0	0.50	−13.09	−13.55

The numerical results were obtained from Greenwald's data using the relation

$$\frac{\partial E_r}{\partial r} = - \frac{\partial E_z}{\partial z} - \frac{E_r}{R} \ .$$

As the table shows, there is a small difference between the plane-geometry approximations and exact calculations due to the curvature of the beam and the conductors in the actual configuration. However, from a practical point of view, the errors are small enough that our analytical approximations are a useful substitute for the numerical method, provided the walls remain close to the ring beam.

5. The Complete Expressions for the Betatron Frequencies

The complete expressions for the betatron frequencies are obtained by including all contributions due to the applied magnetic field, the linear-beam effects, the toroidal or "bias" terms, and the image terms in the formulas (20) and (21) for ν_r^2 and ν_z^2.

The gradient term due to the applied magnetic field can be calculated as follows:

$$(48) \qquad \frac{Rv_\Theta}{E_r + v_\Theta B_z} \frac{\partial B_z^a}{\partial r} = \frac{R}{B_z^a} \frac{\partial B_z^a}{\partial r} \frac{v_\Theta B_z^a}{E_r + v_\Theta B_z} = -n \frac{v_\Theta B_z^a}{E_r + v_\Theta B_z}$$

where

$$(49) \qquad n = - \frac{R}{B_z^a} \frac{\partial B_z^a}{\partial r}$$

is the field index for the applied field at the equilibrium radius $r = R$.

The total field $E_r + v_\Theta B_z$ in the denominator of (48) is the sum of applied and image fields at $r = R$.

$$(50) \qquad E_r + v_\Theta B_z = v_\Theta B_z^a + E_r^i + v_\Theta B_z^i$$

In our plane-geometry approximation, with inner and/or outer conducting boundaries close to the beam, we can neglect the toroidal or "bias" term in the expressions for the betatron frequencies that are generally used. From (50) follows

$$(51) \qquad \frac{v_\Theta B_z^a}{E_r + v_\Theta B_z} = 1 - \frac{(E_r^i + v_\Theta B_z^i)}{E_r + v_\Theta B_z}$$

The image term in (51) depends again on the specific choice of conductor and squirrel cage combinations. From Eqs. (25), (28), (31), (34), (37) and (41), one obtains expressions of the form

$$(52) \qquad \frac{E_r^i + v_\theta B_z^i}{E_r + v_\theta B_z} = \frac{v}{\gamma} \Delta_o^i$$

The parameter Δ_o^i is given as follows.

A. Squirrel cage outside, conductor inside

$$(53) \qquad \Delta_o^i = \frac{\pi(1-f)}{\beta^2(S-T)} \cot \pi \frac{1-T}{S-T} - \frac{1}{1-T}$$

B. Squirrel cage inside, conductor outside

$$(54) \qquad \Delta_o^i = \frac{\pi(1-f)}{\beta^2(S-T)} \cot \pi \frac{1-T}{S-T} + \frac{1}{S-1}$$

C. Conductor only, outside

$$(55) \qquad \Delta_o^i = -\frac{1-f-\beta^2}{\beta^2(S-1)}$$

D. Conductor only, inside

$$(56) \qquad \Delta_o^i = \frac{1-f-\beta^2}{\beta^2(1-T)}$$

E. Squirrel cage only, outside

$$(57) \qquad \Delta_o^i = -\frac{1-f}{\beta^2(S-1)}$$

F. Squirrel cage only, inside

$$(58) \qquad \Delta_o^i = \frac{1-f}{\beta^2(1-T)}$$

Combining all contributions, we can write v_r^2 and v_z^2 in the following form:

$$(59) \qquad v_r^2 = 1 - n - n\frac{v}{\gamma}\Delta_o^i + \frac{v}{\gamma}(-\Delta_\ell{}^r - \Delta_i)$$

(60) $$\nu_z^2 = n + n \frac{\nu}{\gamma} \Delta_o^i + \frac{\nu}{\gamma}(-\Delta_\ell^z + \Delta_i)$$

The first three terms in (59) and the first two terms in (60) represent the contribution due to the gradient of the applied magnetic field. The first term in the brackets represents the linear-beam effect that would exist in a straight beam ($R \rightarrow \infty$). From reference 6, we obtain

(61) $$\Delta_\ell^r = \frac{4R^2}{a(a+b)} \frac{1-f-\beta^2}{\beta^2}$$

(62) $$\Delta_\ell^z = \frac{4R^2}{b(a+b)} \frac{1-f-\beta^2}{\beta^2}$$

Here, the ring is assumed to have a minor cross section of elliptical shape with semi-axis a in radial direction and semi-axis b in axial direction; R denotes the major radius as before. Note that the symbols a and b have a different meaning here than in the derivations presented in Sections 2 through 4. If $f > 1 - \beta^2$, the linear term is defocusing (negative sign), for $f > 1 - \beta^2$, it is focusing, both in the radial as well as in the axial direction.

For completeness and easy reference, we add the expressions for ν_r^2 and ν_z^2 in the form given by Laslett[7] for the case that the image effects are calculated numerically using Bessel functions.

(63) $$\nu_r^2 = 1 - n - n \frac{\nu}{\gamma}\left[\frac{1-f}{\beta^2} K - \bar{L}\right]$$

$$+ \frac{\nu}{\gamma}\left\{ - \frac{4R^2}{a(a+b)} \frac{1-f-\beta^2}{\beta^2} - 4\left[\frac{(1-f)\varepsilon_{1,E}}{\beta^2(S_E - 1)^2} - \frac{\varepsilon_{1,M}}{(S_M - 1)^2}\right]\right\}$$

64) $$\nu_z^2 = n + n \frac{\nu}{\gamma}\left[\frac{1-f}{\beta^2} K - \bar{L}\right]$$

$$+ \frac{\nu}{\gamma}\left\{ - \frac{4R^2}{b(a+b)} \frac{1-f-\beta^2}{\beta^2} + 4\left[\frac{(1-f)\varepsilon_{1,E}}{\beta^2(S_E - 1)^2} - \frac{\varepsilon_{1,M}}{(S_M - 1)^2}\right]\right\}$$

The difference between these equations and Laslett's original expressions is due to the fact that we dropped the toroidal or "bias" terms for reasons stated

earlier. In addition, we left the β^2 factor in all the terms where it enters while Laslett set $\beta^2 = 1$ in some terms when strong relativistic cancellation occurs. Thus, the above formulas are not restricted to relativistic energies.

The new parameters in (63) and (64) are defined as follows:

$$(65) \qquad K = - \frac{8\pi^2 \epsilon_o R^2}{eN_e} E_r^i \quad \left(\text{or } K = \frac{2\pi R^2}{Q} E_r^i \text{ in cgs units used by Laslett} \right)$$

where $Q = -eN_e$ is the total electron charge in the ring.

$$(66) \qquad \bar{L} = \frac{8\pi^2 R^2}{\mu_o eN_e v_\Theta} B_z^i \quad \left(\text{or } \bar{L} = - \frac{R}{I} B_z^i \text{ in cgs units} \right)$$

where $I = - \frac{eN_e}{2\pi R} v_\Theta$ is the total electron current in the ring. S_E and S_M represent the position of electric and magnetic boundaries, $\epsilon_{1,E}$ and $\epsilon_{1,M}$ the electric and magnetic image coefficients. If only one conductor is present outside of the ring, for instance, the two coefficients are defined by Laslett as follows (in cgs units):

$$(67) \qquad \epsilon_{1,E} = \frac{\pi (R_2 - R)^2 R}{2Q} \left(- \frac{\partial E_z}{\partial z} \right) = \frac{\pi R^3 (S-1)^2}{2Q} \left(- \frac{\partial E_z}{\partial z} \right)$$

and

$$(68) \qquad \epsilon_{1,M} = \frac{R^2 (S-1)^2}{4I} \left(- \frac{\partial B_r}{\partial z} \right)$$

with $S_E = S_M = S = \frac{R_2}{R}$. If the conductor is inside the ring, $(S-1)$ is to be replaced by $(1-T)$. If the conductor is replaced by a squirrel cage, $\epsilon_{1,M}$ is practically negligible. With the definitions of (67) and (68), the gradient terms in the formula for v_z^2 may be written in the form

$$(69) \qquad \frac{R \frac{\partial E_z}{\partial z}}{E_r + v_\Theta B_z} = \frac{v(1-f)}{\gamma \beta^2} \, 4 \, \frac{\epsilon_{1,E}}{(S-1)^2} \;,$$

$$(70) \qquad \frac{R \frac{\partial B_r}{\partial z}}{E_r + v_\Theta B_z} = - \frac{v}{\gamma \beta^2} \, 4 \, \frac{\beta^2 \epsilon_{1,M}}{(S-1)^2} \;,$$

which explains the image terms in Eqs. (63) and (64). In the case where only a squirrel cage outside of the ring is present, the plane-geometry approximation yielded the result (44) for the image contribution. By comparison with (69), we see that $\varepsilon_{1,E} = 1/8$, which is in agreement with Laslett's results.[7]

For the case where two conductors or a conductor and a squirrel cage are present, both Greenwald[4] and Hofmann[3] defined $\varepsilon_{1,E}$ and $\varepsilon_{1,M}$ such that $S_E = S_M = S = R_2/R$ = ratio of outer wall boundary to major ring radius.

Acknowledgments

References

1. G. B. Dolbilov et al., Focusing of an Electron Ring in a Collective Linear Ion Accelerator by a System of the Squirrel Cage Type, P9-4737, Dubna, USSR, 1969.

2. L. Jackson Laslett, Current Understanding of ERA, IEEE Trans. NS-$\underline{20}$, 271 (1973).

3. I. Hofmann, Focussing of an Electron Ring in the Presence of a Squirrel Cage and Conducting Cylinder, Technical Report IPP 0/16 (1973), Max-Planck-Institut f. Plasmaphysik, Garching. W. Germany.

4. A. Greenwald, Collective Effects in the Formation and Acceleration of Electron Rings, Ph.D. thesis, PP-76-129 (1975), Dept. of Physics & Astronomy, Univ. of Maryland, College Park, Md. 20742.

5. W. R. Smythe, Static and Dynamic Electricity, Third Edition, McGraw Hill, p. 85.

6. M. Reiser, Part. Accel. $\underline{4}$, 234 (1973).

7. L. Jackson Laslett, On the Focusing Effects Arising from the Self Fields of a Toroidal Beam, ERAN 30 (1969) and ERAN 200 (1972), Lawrence Berkeley Laboratories, California.